

ÉCOLE POLYTECHNIQUE FÉDÉRALE DE LAUSANNE

---

# Conception and optimisation of the electromagnetic shield for the SHIP experiment

---

*Author:*

Alexandre GRANDCHAMP

*Supervisor:*

Federico REDI

*Director:*

Aurelio BAY

June 28, 2018



ÉCOLE POLYTECHNIQUE  
FÉDÉRALE DE LAUSANNE

# Contents

<b>1</b>	<b>Introduction</b>	<b>2</b>
<b>2</b>	<b>The SHiP experiment</b>	<b>2</b>
2.1	Physics motivation . . . . .	4
2.1.1	$\nu$ MSM and the HNL . . . . .	4
2.2	The active muon shield . . . . .	5
2.3	The neutrino detector . . . . .	6
<b>3</b>	<b>Preliminary studies</b>	<b>8</b>
3.1	Necessity of a shield against electromagnetic radiations . . . . .	8
3.2	Simulation framework . . . . .	9
3.3	Implementation of a simple shield . . . . .	9
<b>4</b>	<b>Shape studies</b>	<b>12</b>
<b>5</b>	<b>Shield thickness studies</b>	<b>14</b>
<b>6</b>	<b>Improvement for the downstream detectors</b>	<b>16</b>
<b>7</b>	<b>Future improvements to be made</b>	<b>17</b>
7.1	Grid search for shape optimisation . . . . .	17
7.2	Other improvements considered . . . . .	18
7.2.1	Further shape optimisation . . . . .	18
7.2.2	Density optimisation of the shield . . . . .	18
7.2.3	Study of the energy deposition of electromagnetic particles . . . . .	18
<b>8</b>	<b>Conclusion</b>	<b>19</b>
	<b>Appendices</b>	<b>22</b>
<b>A</b>	<b>Muonic and electromagnetic flux</b>	<b>22</b>
<b>B</b>	<b>Code used</b>	<b>24</b>

# 1 Introduction

With the discovery of the Higgs boson, all the predicted constituents of the Standard Model (SM) have been observed. The SM could therefore possibly be an effective, weakly-coupled field theory up to the Planck scale without the addition of any new particle. However, it leaves some observed phenomena unexplained such as the non-zero neutrino masses, neutrino oscillations and the dark matter and dark energy. These shortcomings of the SM hint at the presence of new physics but provide no clear guidance on its scale or nature.

The SHiP experiment aims to detect hidden particles beyond the SM. Since it targets very weakly interacting particles, it is essential for the experiment to keep the background at a near-zero level. The main source of background being muons, an active muon shield creates a magnetic field to deflect them out of the detectors acceptance. Unfortunately, a part of the deflected muons are interacting with the sides of the active muon shield, initiating electromagnetic showers. These emitted particles are a source of background for the detectors downstream of the active muon shield and especially for the emulsion-based neutrino detector, with the electromagnetic particles risking to spoil its reconstruction capability. It is therefore necessary to shield the detectors from this type of background.

The implementation of a passive shield placed upstream of the neutrino detector and downstream of the active muon shield has been studied here. It aims to reduce the electromagnetic background in the detectors downstream of it, such as the emulsion-based neutrino detector.

## 2 The SHiP experiment

The Super Proton Synchrotron (SPS) is the second largest machine in CERN's accelerator complex. It takes particles from the Proton Synchrotron and accelerates them to provide beams for the Large Hadron Collider (LHC) and fixed target experiments such as the NA61/SHINE and NA62 experiments.

The Search for Hidden Particles (SHiP) experiment is a proposed general purpose fixed target experiment at the CERN SPS. It aims to explore the domain of hidden particles as well as the first experimental measurement of the  $\bar{\nu}_\tau$  interactions and other  $\nu_\tau$  measurements. The particles predicted by hidden portals are expected to be mainly accessible through the decay of heavy hadrons. The SHiP experiment therefore aims to maximise the production and detector acceptance of charm and beauty mesons, while providing a background level compatible with zero.

The primary physics goal of SHiP is to explore hidden portals and extensions of the

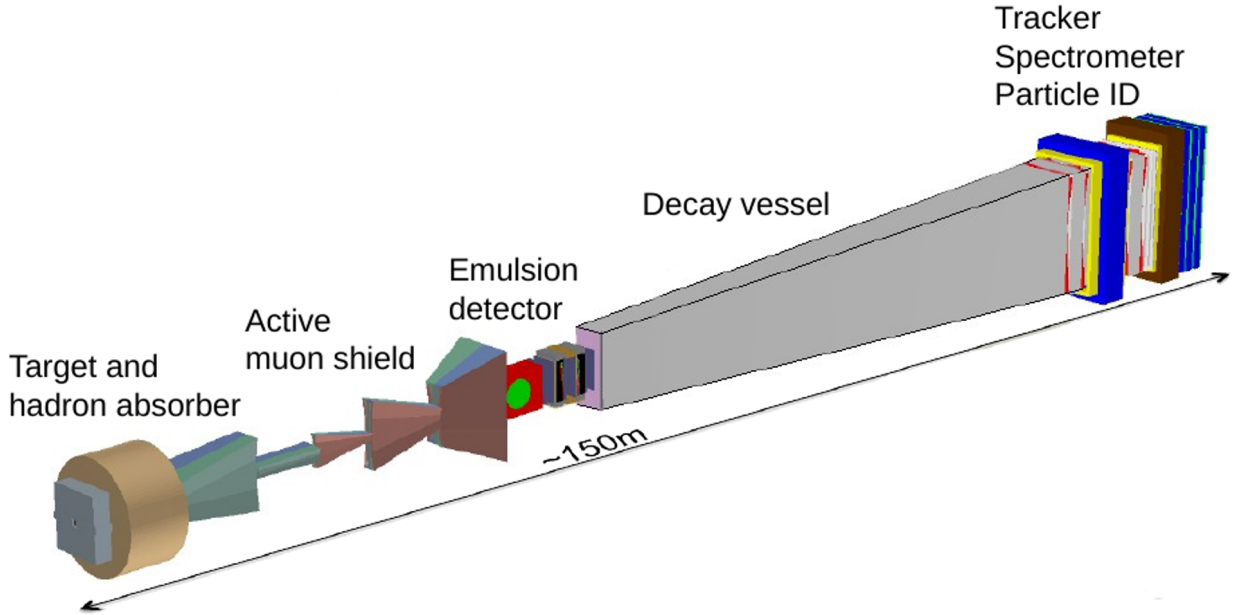


Figure 1: *SHiP experiment beamline, as implemented in the simulation [1].*

SM which incorporate long-lived and very weakly interacting particles through the direct measurement of their decay to SM particles. The experiment will maximise the number of heavy mesons produced ( $8 \cdot 10^{17}$   $D$  mesons are expected in 5 years of operation[2]) since many of the hidden particles are expected to be accessible through heavy hadron decays. The beamline of the experiment can be seen in Figure 1.

A beam of 400 GeV protons will be extracted from the SPS and dumped onto a heavy target with the goal of collecting  $2 \cdot 10^{20}$  Protons On Target (POT) in five years of operation [2]. The target is followed by a hadron stopper to absorb pions and kaons before they decay. An active muon shield then creates a magnetic field deflecting the muons from the fiducial volume. Downstream of it is an OPERA-like [3] emulsion-based neutrino detector placed in a magnetic field which is followed by a muon magnetic spectrometer to identify the muons produced in  $\nu$  and  $\tau$  induced decays. Downstream of it is the Upstream Veto Tagger (UVT), made of plastic scintillator bars, whose goal is to control the background from neutral kaons coming mainly from interactions in the neutrino detector's passive material and to veto muons entering the vessel.

The second part of the facility is dedicated to the hidden particle detector consisting in a 50 m long decay volume surrounded by liquid scintillators, the Surrounding Background Taggers (SBT) which veto charged particles entering the decay volume. The decay volume or vacuum vessel is maintained in a vacuum to limit the number of neutrino interactions in the volume. The Straw Veto Tagger (SVT) is placed 5 m downstream of the decay volume's

entrance and vetoes background induced by interactions in the entrance window of the vacuum vessel. At the end of the decay vessel are located the Hidden Sector (HS) spectrometer, made from a dipole magnet ( $5 \cdot 10 \text{ m}^2$ ) and 4 stations measuring the  $x$  and  $y$  transverse coordinates of the particles and a fifth station to veto the combinatorial background.

Downstream of the HS spectrometer is the spectrometer timing detector, aiming to reduce the di-muon combinatorial background by requiring that the measured signal particles in SHiP spectrometer are coincident in time.

It is followed by an electromagnetic calorimeter, a hadronic calorimeter and a muon detector to identify muons from hidden particle decays [4].

## 2.1 Physics motivation

With the discovery of the Higgs boson by the ATLAS [5] and CMS [6] experiments, all the predicted constituents of the SM have been observed. The SM could therefore possibly be an effective, weakly-coupled field theory up to the Planck scale without the addition of any new particle.

However, a number of phenomena are left unexplained by the SM such as the non-zero mass of the neutrino, the neutrino oscillations [7], the Baryonic Asymmetry of the Universe (BAU) [8] or the existence of Dark Matter and Dark Energy [9]. These shortcomings of the SM hint at the presence of new physics but provide no clear guidance on its scale or nature.

In the search for new physics, the high energy frontier will be investigated at CERN in the years to come with the high luminosity LHC and other circular colliders. In complement to this, the domain of searches at the intensity frontier which consists in looking for processes very weakly coupled to the SM stays largely unexplored and is investigated by experiments such as SHiP. Indeed, the experiment is designed to find particles which would be too weakly coupled to be seen by previous general purpose experiments and with an invariant mass of  $m_{NP} < \mathcal{O}(10 \text{ GeV}/c^2)$  [10]. The experiment will look for light new particles from a wide range of theories such as the dark photon, axion-like particles or Heavy Neutral leptons (HNL).

### 2.1.1 $\nu$ MSM and the HNL

In the neutrino Minimal Standard Model ( $\nu$ MSM), three new fundamental right-handed fermions  $N_{1,2,3}$  are added to the SM. The addition of these new particles makes the leptonic sector similar to the quark sector (Figure 2). In the model described in [11], the lightest HNL,  $N_1$  has a mass in  $\mathcal{O}(10) \text{ keV}$  and would be a DM candidate with a lifetime exceeding

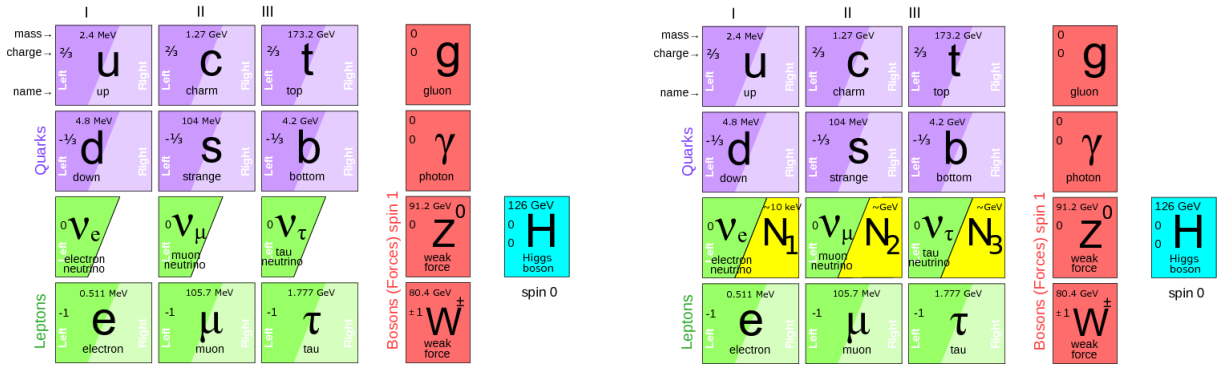


Figure 2: *Small Particle content of the SM and its minimal extension in the neutrino sector. In the (left) SM the right-handed partners of neutrinos are absent. In the (right)  $\nu$ MSM all fermions have both left- and right-handed components and masses below the Fermi scale [12].*

the lifetime of the universe. The other two,  $N_2$  and  $N_3$  have a mass in  $\mathcal{O}(1)$  GeV and could provide an explanation for the neutrino masses and oscillations.

One of the decay modes of  $N_1$  is ( $N \rightarrow \nu\gamma$ ), which can be searched for by looking for a monochromatic line corresponding to the  $\gamma$ . Recent observations [13] may be hinting at this decay.  $N_{2,3}$  can be produced in weak decays of heavy mesons such as the  $D$  meson due to their mixing with the SM neutrinos. They can then decay into SM particles which makes them interesting for experimental studies. The cleanest signature experimentally for the decay of the HNL is the final state  $\mu^-\pi^+$  [12]. The SHiP experiment will thoroughly explore the phase space for such decays [4].

## 2.2 The active muon shield

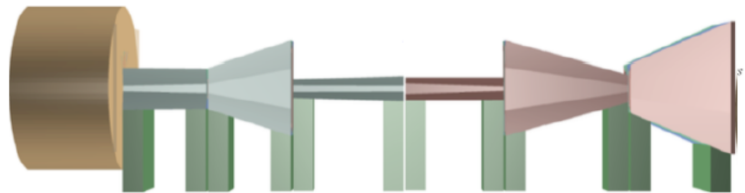


Figure 3: *Baseline configuration of the SHiP muon shield. [14]*

A critical component of the SHiP experiment is the active muon shield since it deflects the high flux of muons produced in the target, which would represent a serious background for the particle searches. The first region of the active muon shield is designed to separate the  $\mu^+$  and  $\mu^-$  so that they are bent to opposite directions independently of their initial trajectory and are deflected from the detectors acceptance.

Since there is a large spread of the muons phase space, the return field of the magnet tends to bend the low momentum muons ( $\sim 50$  GeV/c) back towards the spectrometer.

To solve this problem, the second region consists in a second magnet with an opposite polarity field which will bend further outward the high momentum muons ( $\sim 350$  GeV/c) and deflect back the low momentum muons which were affected by the return field.

A simple schematic view of the effect of the active muon shield on the muons is provided in Figure 4.

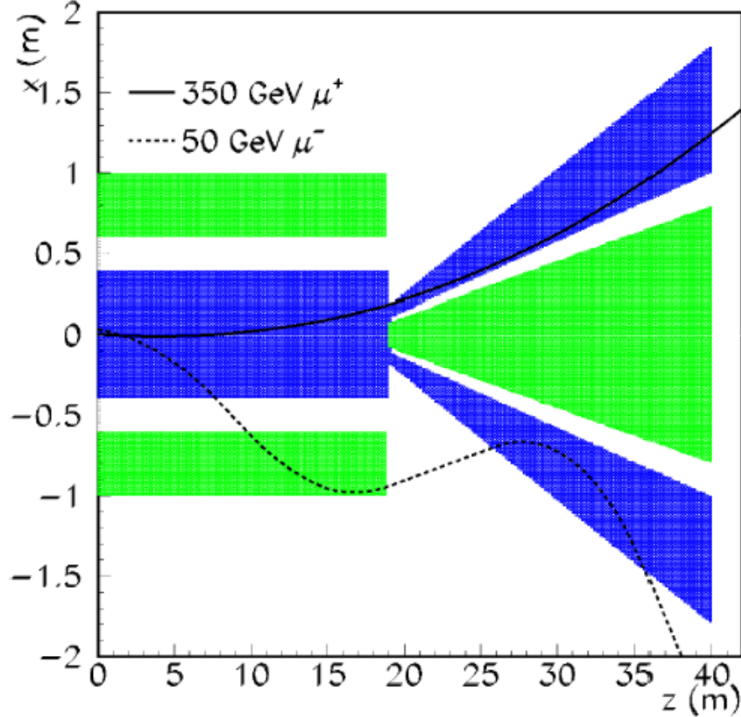


Figure 4: *Cross section at  $y = 0$  shows the principle of magnetic shielding. The magnetic field is along the  $y$ -axis, and its polarity is indicated by the blue/green color of the iron poles of the magnets. The trajectories of a 350 GeV/c muon and 50 GeV/c muon are shown with a full and dashed line, respectively. [15]*

### 2.3 The neutrino detector

The neutrino detector is located directly downstream of the active muon shield and is designed to perform the first direct detection of the  $\bar{\nu}_\tau$  and study the properties and cross-sections of  $\nu_\tau$  and  $\bar{\nu}_\tau$ . It is also well suited to search for Light Dark Matter (LDM) particles produced by the decay of the dark photon and scattered off electrons [16]. The neutrino detector is constituted of an emulsion target placed in a magnet and electronic detectors (the

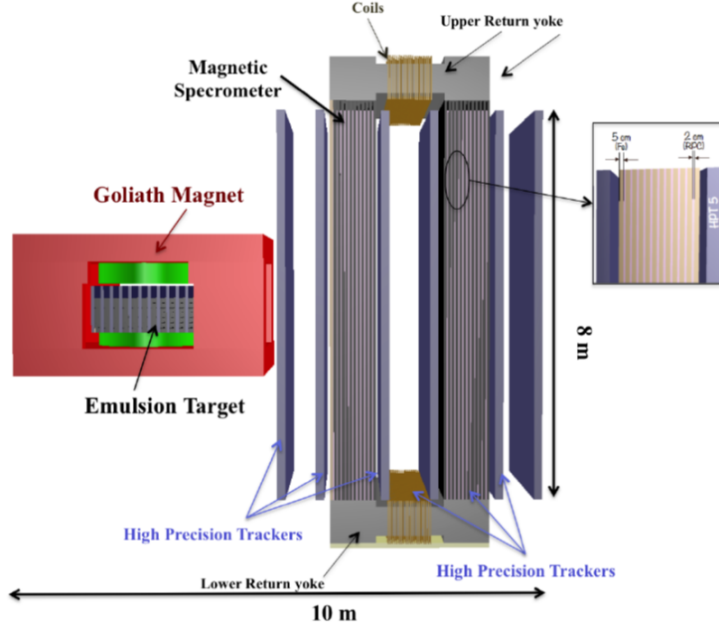


Figure 5: *Layout of the emulsion detector: the emulsion target is placed inside the Goliath Magnet and it is followed downstream by a muon magnetic spectrometer. [16]*

Target Trackers). It is followed by the muon magnetic spectrometer. Figure 5 shows the near detector area, constituted of the neutrino detector and the muon magnetic spectrometer.

As described in [16], the emulsion films consists in two active layers of  $44\ \mu\text{m}$  with a plastic base of  $205\ \mu\text{m}$  in between the two. The active layer is constituted of silver bromide (AgBr) crystals in a gelatine binder. When a charged particles goes through the active layer, electron-holes pairs are formed, which leads to the production of Ag atoms visible on an optical microscope.

The emulsion films are used for the Emulsion Cloud Chambers (ECC), which are constituted of 57 emulsion films interleaved by 56 lead plates, for a total length of 79mm and for the Compact Emulsion Spectrometer (CES), located directly downstream of the ECC and made from 3 emulsion films separated by two plates 1.5 mm thick plates of light material (Rohacell structural foam).

The goal of the CES is to measure the electric charge of the particles emitted by the  $\tau$  decay to distinguish between  $\nu_\tau$  and  $\bar{\nu}_\tau$  interactions. As shown in Figure 6, a unit is made of an ECC brick followed by a CES.

The emulsion target is constituted of 11 walls with 105 units per wall. The walls are interleaved with electronic detectors (the Target Trackers) used to provide the timestamp to a reconstructed event.

The so called Goliath magnet surrounds the emulsion target and the Target Trackers and

provides a field higher than 1 T in the region of the emulsion target, which is necessary to perform the electric charge measurements.

This is only a preliminary iteration and a different magnet will probably be used for the final design. The electromagnetic shield can however be easily be redefined in the simulation to accommodate this change in design. Indeed since its shape is simple the optimisation procedure can be automatised to account for the change in design of the emulsion detector.

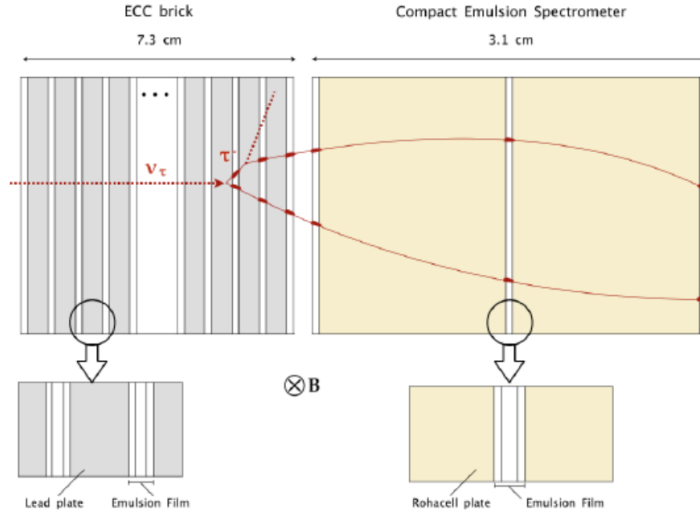


Figure 6: *Schematic representation of the target unit: the Brick and the CES [16].*

### 3 Preliminary studies

#### 3.1 Necessity of a shield against electromagnetic radiations

During the studies conducted for the active muon shield optimisation [15], it was found that a large flux of low energy electrons and photons is produced by the muons hitting the magnets in addition with those emitted directly at the target. They constitute an additional source of background for the SBT surrounding the SHiP vessel, which are designed to tag any charged particle entering the vessel.

Moreover, as it can be seen on Figure 7 the number of electromagnetic particles hitting the UVT is greatly reduced when the emulsion-based detector and the muon magnetic spectrometer are present, which indicates that these detectors currently act as a shielding against electromagnetic radiation for the downstream detectors. Therefore, the low energy electrons are spoiling the reconstruction capability of the emulsion target [15]. The flux of those electromagnetic particles therefore needs to be controlled.

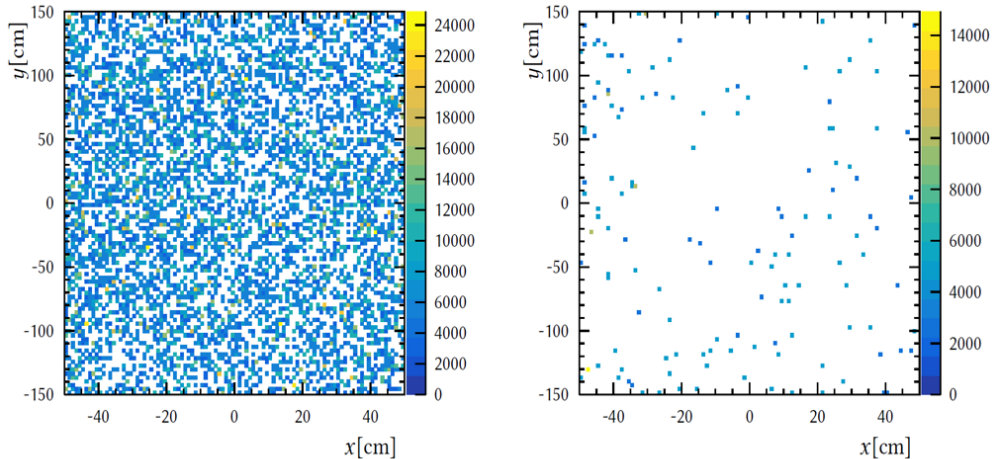


Figure 7: *Close-up of the hits distribution for the UVT without and with the emulsion-based neutrino detector and the muon magnetic spectrometer implemented upstream of it [17].*

### 3.2 Simulation framework

The SHiP simulation and reconstruction software is based on the FairRoot [18] framework which is fully based on the ROOT system and provides base classes for detector construction with the ROOT package TGeo and for analysis tasks. Specific libraries needed by SHiP are added to this framework to form the FairShip framework.

The events for physics performance studies are produced by the Monte Carlo generators. PYTHIA8 [19] is used for the simulation of the proton collisions with SHiP target, PYTHIA6 [20] for the inelastic muons interactions and GEANT4 [21] to simulate the SHiP detector response.

For the following studies, the MuonBack simulation engine is used to generate events from the muon background file. This file contains 18 million muons generated with PYTHIA8. On the one hand, the number of events simulated using the MuonBack generator correspond to the number of muons generated after the target. On the other hand, the weights applied to the reconstructed hits (see Subsection 3.3, Section 4 and Section 5) refer to the POT delivered in one spill.

In the simulation, the  $z$  axis is along the beamline and is positively defined in the downstream direction, with  $x$  and  $y$  respectively defined horizontally and vertically.

### 3.3 Implementation of a simple shield

Since the emulsion detector needs to be shielded from the electromagnetic radiations created at the end of the muon shield, the location chosen for the electromagnetic shielding is in

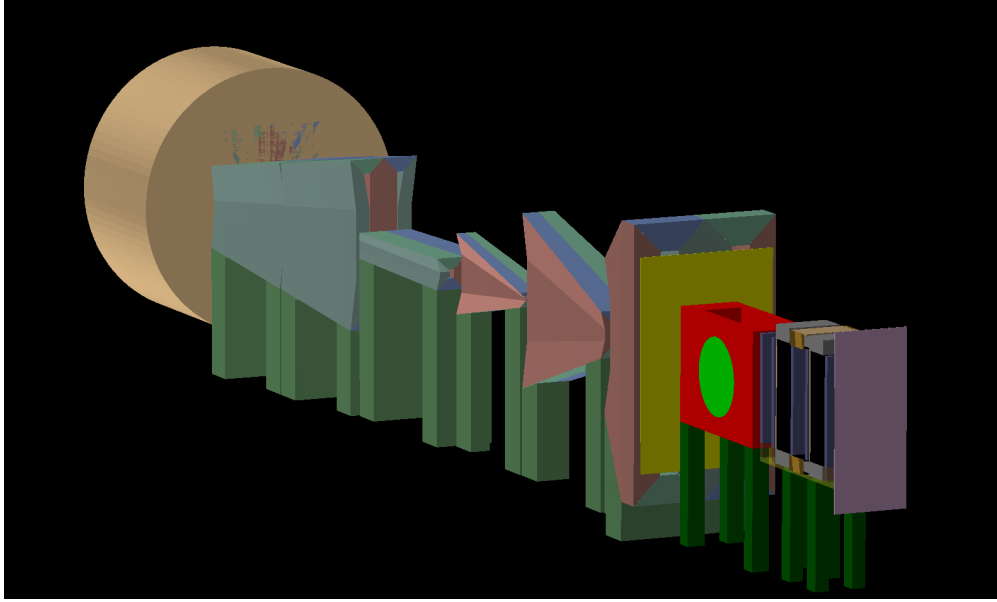


Figure 8: *Representation of the active muon shield, followed by a box shaped electromagnetic shielding (yellow) and the near detector region*

between the active muon shield and the neutrino detector, as it can be seen in Figure 8.

The first goal of this study is to understand the shape of the muon flux distribution directly after the active muon shield. Indeed, the muons interacting in the lead shielding have a chance to initiate electromagnetic showers. Therefore, placing the shield in a region where the muon flux is dense would lead to more electromagnetic shower being initiated and therefore more background for the emulsion detector downstream.

Lead has been chosen as a medium for the shield and, in order to understand the shape of the muon flux distribution it has been implemented with a bigger width and height than what is believed necessary. Its dimensions are  $500 \cdot 600 \cdot 4 \text{ cm}^3$ .

A simulation of  $10^5$  events using the MuonBack generator has been performed. The distribution of the muon interactions in the electromagnetic shield can be observed in Figure 9. The events have been weighted to correspond to one spill (i.e.  $4 \cdot 10^{13}$  POT [16]). The absence of muon interactions in the central region comes from the fact that the active muon shield is deflecting the  $\mu^+$  and  $\mu^-$  along the  $x$  axis. The spread of the distribution at low values of  $y$  is due to the return field of the magnets.

Since the number of muon interactions in the electromagnetic shield needs to be minimised, the area where the muon flux is too dense is avoided when implementing the shield. A rough representation of this area is shown in Figure 10.

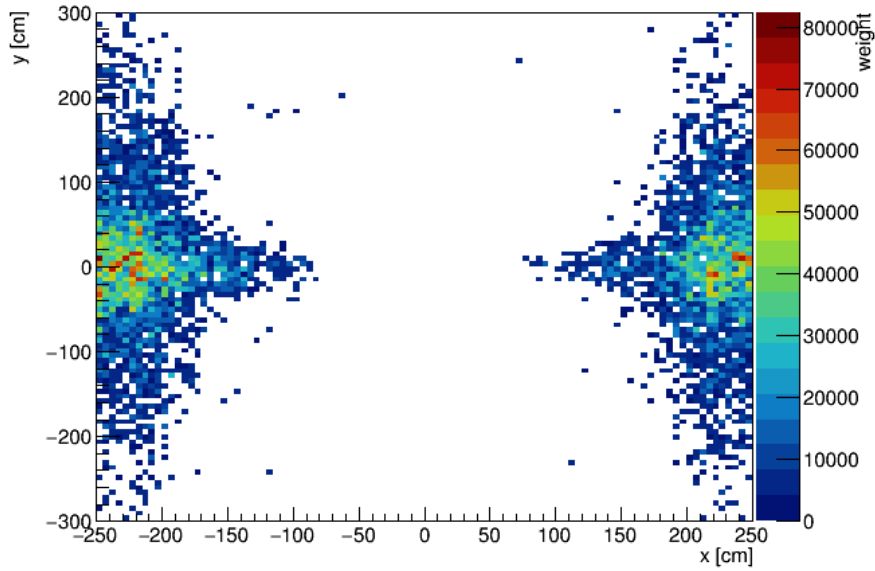


Figure 9: *Weighted number of muons hitting the box-shaped 4 cm thick lead shield as a function of  $x$  and  $y$ . The events are weighted to one spill of  $4 \cdot 10^{13}$  POT.*

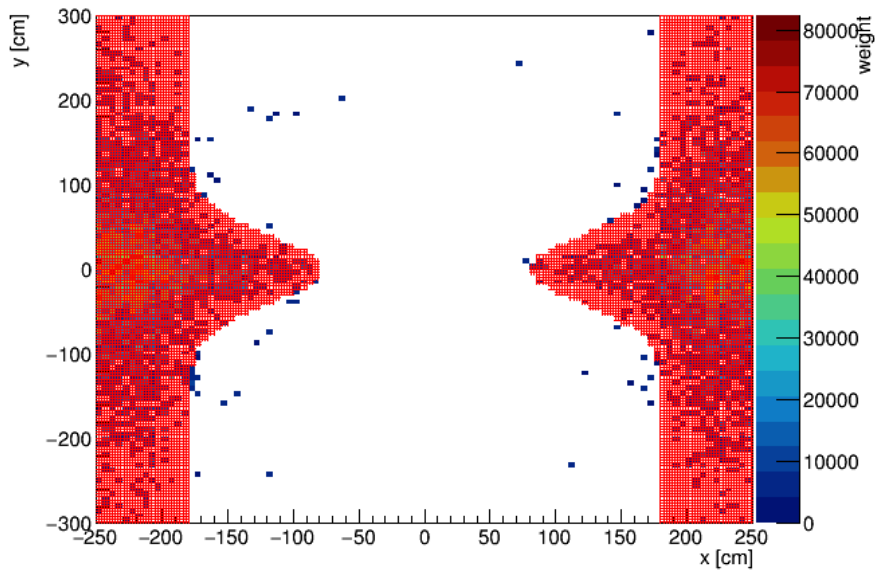


Figure 10: *Weighted number of muons hitting the box-shaped 4 cm thick lead shield as a function of  $x$  and  $y$ . The events are weighted to one spill of  $4 \cdot 10^{13}$  POT. The area where the muon flux is too dense to implement a lead shield is shown in red.*

## 4 Shape studies

Given the muon flux distribution described in Subsection 3.3 and the necessity to avoid muon interactions in the electromagnetic shield, a hourglass shape was considered for the shielding. The hourglass is constituted of two trapezoids for the central region and two rectangles for the outer region. The resulting shape can be seen in Figure 11. The medium used for the electromagnetic shielding remains lead and the thickness is still set to 4 cm. The height and width of the rectangles are respectively 2 m and 3.2 m, whereas each of the trapezoids is 1 m high. Two different shapes were studied, respectively with a 2 m and 1.6 m width at the centre. The simulations were made using  $10^5$  events from the MuonBack generator.

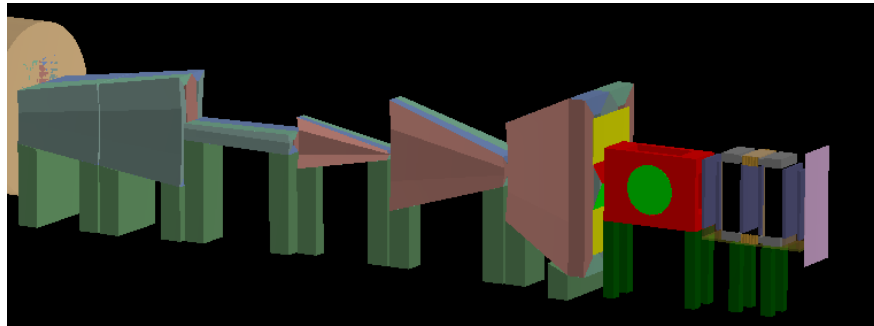


Figure 11: *Representation of the near detector area including the hourglass shaped electromagnetic shield constituted of two trapezoids (red and green) and two rectangles (yellow).*

For the shield design with a 2 m width in the centre, the distribution of muon hits in the electromagnetic shield resulting from the simulation is shown in Figure 12. A reduction in the number of muon interactions in the shield can be noticed in comparison with the rectangular shape considered at first, but a concentration of muon interactions at the edges of the central region of the shield is still present. This indicates that the muon flux is not fully avoided with this shield design and a narrower shield should be considered in order to avoid initiating too many electromagnetic showers in it.

For the narrower shield (1.6 m wide at the centre), the distribution of muon hits is shown in Figure 13. One can notice that the number of muons interacting in the shield has been greatly reduced, from  $73 \pm 9$  to  $30 \pm 5$  for  $10^5$  events simulated. Moreover, the pattern observed for the wider shield does not appear at the edges of the central region, meaning that the shape considered is narrow enough to fully avoid the region where the muon flux is dense. Therefore, the number of muon interactions is limited and so is the number of electromagnetic showers initiated.

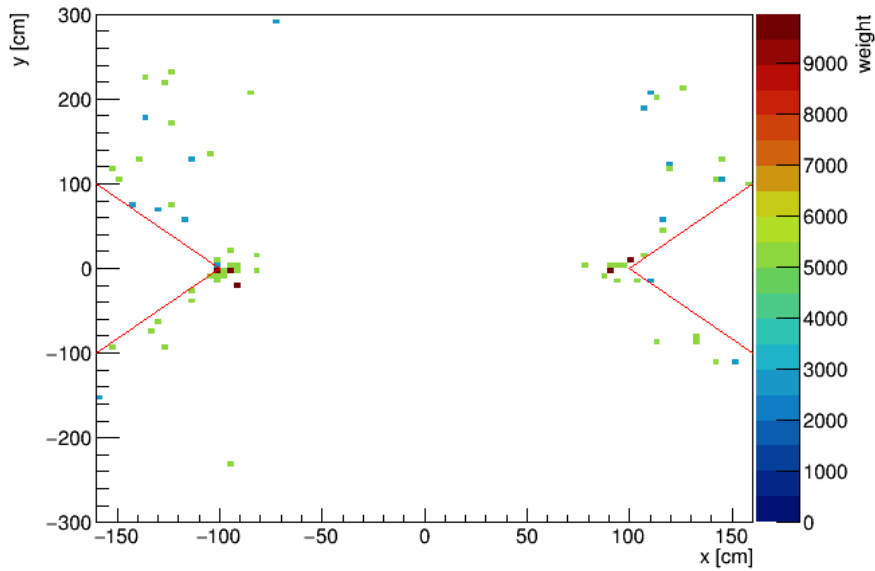


Figure 12: *Weighted number of muons hitting the electromagnetic shielding as a function of  $x$  and  $y$ . The events are weighted to one spill of  $4 \cdot 10^{13}$  POT. The electromagnetic shield is 2 m wide at the centre and its limits are shown by the red lines.*

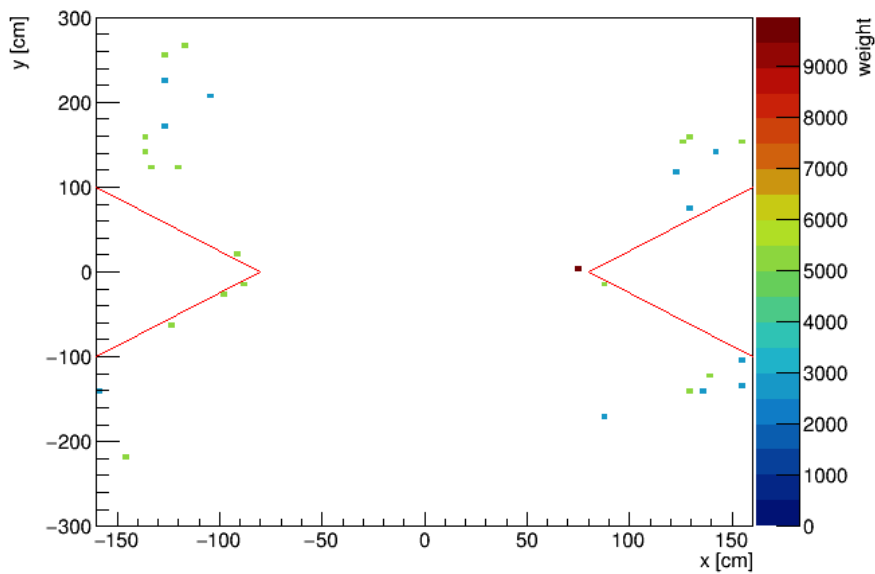


Figure 13: *Weighted number of muons hitting the electromagnetic shielding as a function of  $x$  and  $y$ . The events are weighted to one spill of  $4 \cdot 10^{13}$  POT. The electromagnetic shield is 1.6 m wide at the centre and its limits are shown by the red lines.*

## 5 Shield thickness studies

After the appropriate shape has been chosen, the question of the thickness has been addressed. To do so, the shield in the simulation was implemented as successive lead layers with a thickness of 5 mm, interleaved with 1 mm active vacuum layer whose role is to count and identify the particles going through it. The shape of the lead layers has been defined as the hourglass shape with a 1.6 m width for the central region, as discussed in Section 4. The sensitive layers have a surface of  $520 \cdot 800 \text{ cm}^2$ . This design can be observed in Figure 14.

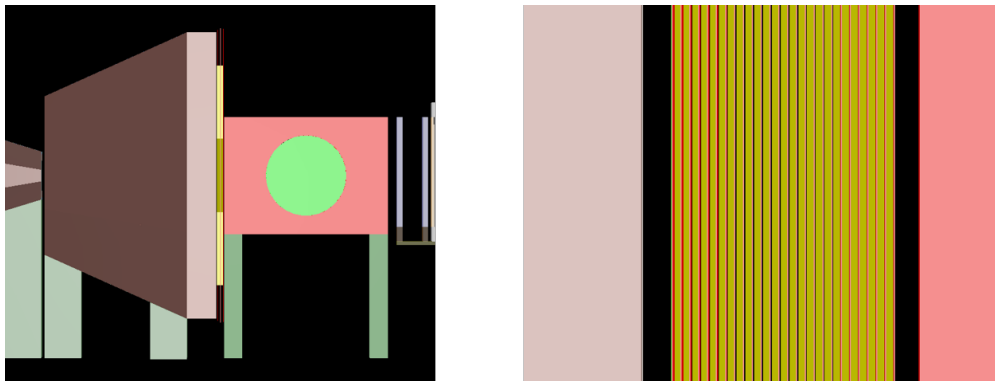


Figure 14: *Representation of the layered design of the electromagnetic shield with the hourglass shaped lead layers (yellow) and the vacuum sensitive volumes (red)*

The purpose of this implementation is to study the effects of a varying shield thickness on the number of electromagnetic particles stopped by or crossing the shield. Of course, the final design of the shield will be made of a single layer. As previously stated, the simulations are made using  $10^5$  events from the MuonBack generator.

The number of electromagnetic hits in the shield in terms of its thickness and the number of electromagnetic particles remaining as a function of the shield thickness are shown in Figure 15 and Figure 16 respectively.

The figures show that both the number of electromagnetic hits in the shield and the number of electromagnetic particles after it quickly fall to numbers close to zero after a few centimetres of lead. Indeed, only 5 cm are enough for the number of electromagnetic particles after the shield to become statistically insignificant.

In both cases, it can also be noticed that the number of electromagnetic particles continues to fluctuate even when the shield becomes thick. This can be explained by the presence of residual muons which have not been deflected by the active muon shield. These muons interact in the shield and initiate electromagnetic showers, resulting in the fluctuations seen on the previous distributions. It is not possible to counter this effect with a few centimetres of lead.

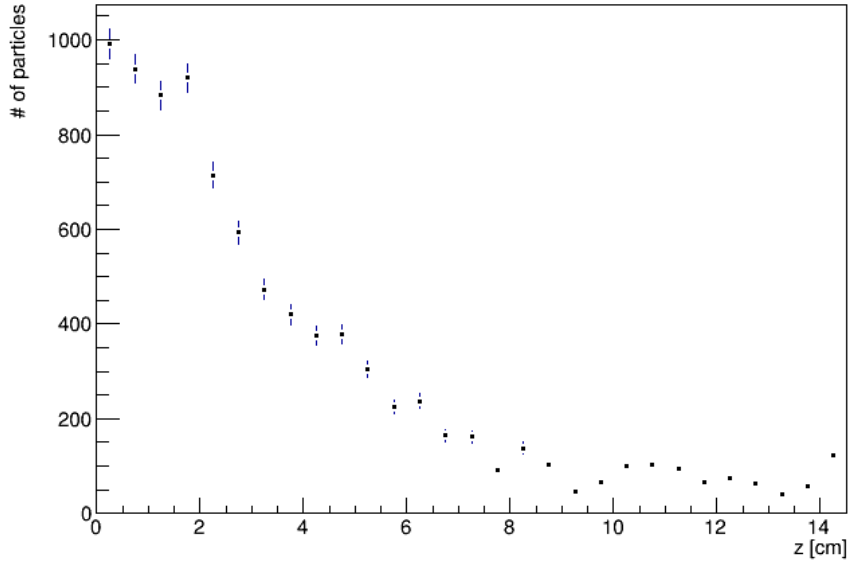


Figure 15: *Number of electromagnetic particles hitting a hourglass-shaped lead shield as a function of its thickness*

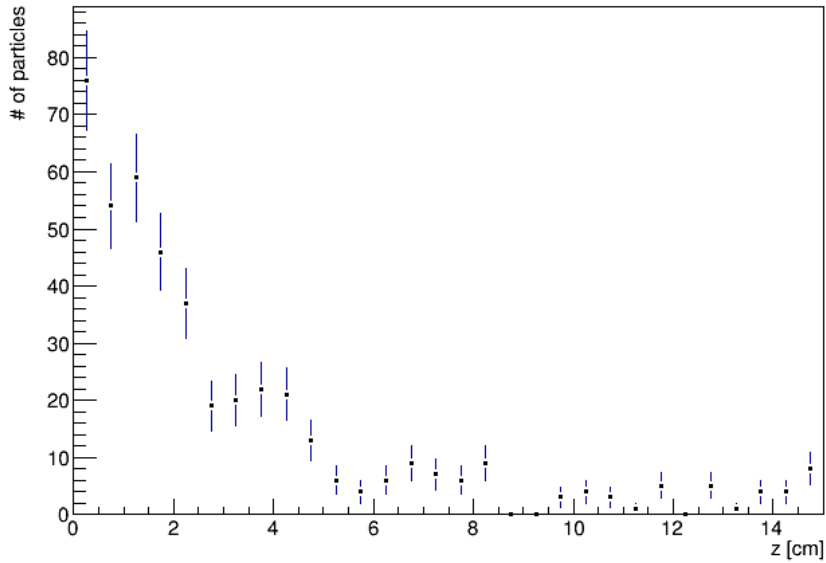


Figure 16: *Number of electromagnetic particles remaining after a hourglass-shaped lead shield as a function of the shields thickness*

## 6 Improvement for the downstream detectors

The effect of the presence of the electromagnetic shield on the emulsion detector has been studied. A 2.5 cm thick lead shield with the hourglass shape chosen in Section 4 has been considered for this simulation.

Due to time constraints for this project, the simulation of the full number of events ( $1.8 \cdot 10^7$ ) was not possible. The volume of interest (the  $77 \cdot 150 \cdot 188 \text{ cm}^3$  box inside the Goliath magnet) was therefore replaced for this simulation by a lead box. This way, the number of interactions in the volume is artificially increased compared to the case with the emulsion.

This substitution allows to study the electromagnetic background reduction in the area of the emulsion detector even with a limited number of simulated events.  $5 \cdot 10^5$  events from the MuonBack generator were used.

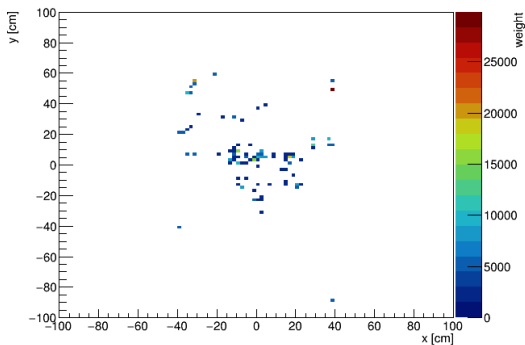


Figure 17: *Weighted number of particles hitting the emulsion detector as a function of  $x$  and  $y$ . The events are weighted to one spill of  $4 \cdot 10^{13}$  POT. No electromagnetic shielding is in place and the volume of the emulsion detector is replaced by a lead box.*

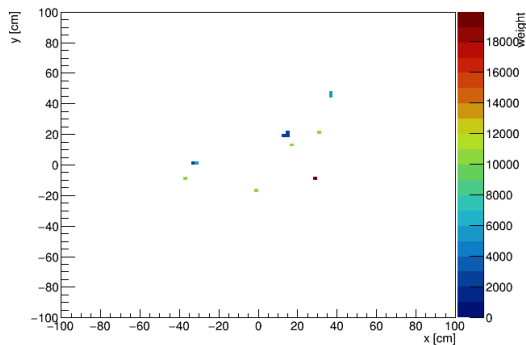


Figure 18: *Weighted number of particles hitting the emulsion detector as a function of  $x$  and  $y$ . The events are weighted to one spill of  $4 \cdot 10^{13}$  POT. A lead, hourglass-shaped electromagnetic shielding is in place and the volume of the emulsion detector is replaced by a lead box.*

Figure 17 and Figure 18 show the representation of the hits in the transverse plane ( $x, y$ ) in the volume of interest without and with the 2.5 cm thick electromagnetic shield placed upstream. The reduction of the number of particles interacting in the volume clearly appears (from  $151 \pm 12$  to  $20 \pm 4$  hits). However, it could be argued that defining the volume as a lead box is not optimal since a muon interacting in the volume could initiate an electromagnetic

shower and would spoil the measurement by artificially introducing an important number of extra particles.

To get rid of this effect, the simulation was made again with the difference that the volume of interest was this time defined in the simulation as a vacuum sensitive volume similar to the layers introduced in Section 5, This allows to count the number of particles going through the volume instead of the number of interactions. A number of  $10^6$  events from the MuonBack generator have been used for this simulation. The result of this study show a decrease in the number of particles entering the volume, from 9 without the shield to 1 with the 2.5 cm thick shield. However, a simulation with more statistics is needed to have a quantitative estimate.

## 7 Future improvements to be made

### 7.1 Grid search for shape optimisation

It is planned to optimise the electromagnetic shielding using a “grid search” method. Up to 6 parameters can be considered for the hourglass shaped shield, namely the height and width of the rectangular parts, the height and central width of the trapezoidal part along with the thickness and density of the shield.

The range of most of the parameters will be limited by the region where the muon flux is dense since the muon interactions need to be minimised in the shield. A lower limit on the dimensions of the shield can also be set since the distribution electromagnetic particles is close to the muon flux. As a result, it would not be interesting to have a shield that is too small and thus too far away from the muon flux region since it would also shield fewer electromagnetic particles.

Therefore, the upper and lower limits for the range of some of the parameters can be established in the light of the studies previously conducted. Concerning the width of the central region, it has been seen in Section 4 that 2 m was already too wide while 1.6 m did not pose any problem regarding the muon interactions in the shield. Therefore the range to be explored could be from 1.4 to 2.2 m for instance.

It also wouldn't be useful to set smaller value than 50 cm for the height of each trapezoid. Indeed, 50 cm high trapezoids would already bring the edge of the shield very close to the muon flux region and it can therefore be considered as the minimal value.

It has been seen in the Section 4 that the number of electromagnetic particles remaining after the shield falls to values consistent with zero after a 5 cm thick lead shield. A maximal value could therefore be slightly over this value, 7 cm for instance. Of course if one is varying

the density and the thickness at the same time, the values would need to be adapted. For instance, if 7 cm is the maximal thickness for a lead shield, the corresponding thickness for a tungsten shield should then be lower. The interaction length may be considered as a parameter instead of the thickness.

## **7.2 Other improvements considered**

A number of studies could be conducted to further optimize the efficiency of the shield.

### **7.2.1 Further shape optimisation**

The shape which has been chosen during this project is constituted of two rectangles for the outer regions and two trapezoids at the centre, the goal being to avoid placing the lead shield in the area where the muon flux is too dense. However, the area avoided by the trapezoids is only an approximation of the real shape of the muon flux, which can be seen in Figure 9. A possible improvement could therefore better follow the muon flux distribution in the central region of the shield, by excluding a “Gaussian-shaped” area on the sides of the shield. With this solution, a greater number of electromagnetic particles could be stopped while reducing as much as possible muon interactions.

### **7.2.2 Density optimisation of the shield**

A more complex implementation would be to consider the shield not as a single block but as made of a number of small blocks with densities to optimise for the best background suppression. It would allow to reduce the number of muon hits by considering a lower density in the regions where muons interact while shielding the detectors downstream as much as possible. If proven useful, this variable density could be made possible by using tungsten with varying alloys proportion.

Another possibility would be to consider a variable thickness of the shield instead of a variable density.

### **7.2.3 Study of the energy deposition of electromagnetic particles**

During this project, the main criterion to evaluate the background was to consider the number of electromagnetic particles interacting in the detectors volume. However it would be interesting to study the energy deposition of the electromagnetic particles in the different subdetectors. Indeed, the focus should be on the most energetic particles and it would therefore be necessary to look at the energy depositions to understand which particles are

the most problematic and thus which particles need to be shielded the most. This would allow to design a more appropriate shape for the shield.

## 8 Conclusion

The effect of a passive shield on the electromagnetic background for the downstream detectors in the SHiP experiment has been studied.

It has been found that because of the particular shape of the muon flux distribution, a hourglass-shape as described in Section 4 would be the most appropriate to avoid the production of electromagnetic showers from the muon interactions in the shield. The thickness needed was found to be 5 cm to be able to shield most of the electromagnetic particles. A positive effect of the shield on the background level for the emulsion-based neutrino detector using lead was also demonstrated.

It is now necessary to increase the number of events simulated a more detailed study to improve further the efficiency of the shield, as seen in Subsection 7.2.

A grid search optimisation of the shape and thickness has been proposed, as well as a further shape optimisation and an optimisation based on density adjustment of the shield. A study of the energy deposition of the electromagnetic particles in the different detectors would also be interesting to target more efficiently the most problematic particles.

## References

- [1] SHiP collaboration, P. Mermoud, *Right-handed neutrinos: the hunt is on!*, Tech. Rep. [1704.08635], Apr, 2017.
- [2] SHiP collaboration, M. Anelli et al., *A Facility to Search for Hidden Particles (SHiP) at the CERN SPS*, Tech. Rep. CERN-SPSC-2015-016. SPSC-P-350. [1504.04956], CERN, Geneva, Apr, 2015.
- [3] D. Di Ferdinando, *Nuclear emulsions in the OPERA experiment*, *Radiation Measurements* **44** (2009) 840 [0812.0451].
- [4] SHiP collaboration, S. Alekhin et al., *A facility to Search for Hidden Particles at the CERN SPS: the SHiP physics case*, Tech. Rep. CERN-SPSC-2015-017. SPSC-P-350-ADD-1, CERN, Geneva, Apr, 2015.
- [5] ATLAS collaboration, G. Aad et al., *Observation of a new particle in the search for the Standard Model Higgs boson with the ATLAS detector at the LHC*, *Phys.Lett.* **B716** (2012) 1 [1207.7214].
- [6] CMS collaboration, *Combination of standard model Higgs boson searches and measurements of the properties of the new boson with a mass near 125 GeV*, Tech. Rep. CMS-PAS-HIG-13-005, CERN, Geneva, 2013.
- [7] KAMLAND collaboration, K. Eguchi et al., *First results from KamLAND: Evidence for reactor anti-neutrino disappearance*, *Phys. Rev. Lett.* **90** (2003) 021802 [hep-ex/0212021].
- [8] A. D. Sakharov, *Violation of CP Invariance, C asymmetry, and baryon asymmetry of the universe*, *Pisma Zh. Eksp. Teor. Fiz.* **5** (1967) 32.
- [9] PARTICLE DATA GROUP collaboration, C. Patrignani et al., *Review of Particle Physics*, *Chin. Phys.* **C40** (2016) 100001.
- [10] O. Lantwin, *Search for new physics with the SHiP experiment at CERN*, *PoS EPS-HEP2017* (2017) 304 [1710.03277].
- [11] T. Asaka, S. Blanchet and M. Shaposhnikov, *The  $\nu$ MSM, dark matter and neutrino masses*, *Phys. Lett.* **B631** (2005) 151 [hep-ph/0503065].
- [12] W. Bonivento et al., *Proposal to Search for Heavy Neutral Leptons at the SPS*, Tech. Rep. CERN-SPSC-2013-024. SPSC-EOI-010, CERN, Geneva, Oct, 2013.

- [13] E. Bulbul, M. Markevitch, A. Foster, R. K. Smith, M. Loewenstein and S. W. Randall, *Detection of An Unidentified Emission Line in the Stacked X-ray spectrum of Galaxy Clusters*, *Astrophys. J.* **789** (2014) 13 [1402.2301].
- [14] A. Baranov, E. Burnaev, D. Derkach, A. Filatov, N. Klyuchnikov, O. Lantwin et al., *Optimising the active muon shield for the SHiP experiment at CERN*, *Journal of Physics: Conference Series* **934** (2017) 012050.
- [15] SHiP collaboration, A. Akmete et al., *The active muon shield in the SHiP experiment*, *JINST* **12** (2017) P05011 [1703.03612].
- [16] A. Buonauro, *Study of  $\nu_\tau$  properties with the SHiP experiment*, Ph.D. thesis, Università degli studi di Napoli "Federico II", 2017.
- [17] O. Lantwin. personal communication, Mar., 2018.
- [18] M. Al-Turany, D. Bertini, R. Karabowicz, D. Kresan, P. Malzacher, T. Stockmanns et al., *The FairRoot framework*, *J. Phys. Conf. Ser.* **396** (2012) 022001.
- [19] T. Sjostrand, S. Mrenna and P. Z. Skands, *A Brief Introduction to PYTHIA 8.1*, *Comput. Phys. Commun.* **178** (2008) 852 [0710.3820].
- [20] T. Sjostrand, S. Mrenna and P. Z. Skands, *PYTHIA 6.4 Physics and Manual*, *JHEP* **05** (2006) 026 [hep-ph/0603175].
- [21] GEANT4 collaboration, S. Agostinelli et al., *GEANT4: A Simulation toolkit*, *Nucl. Instrum. Meth.* **A506** (2003) 250.

# Appendices

## A Muonic and electromagnetic flux

To get a better representation of the particle flux after the active muon shield, a sensitive vacuum area similar to the ones described in Section 4 was implemented in the simulation. This way, a representation of the muon flux distribution can be established, as shown in Figure 20. More importantly the flux of electromagnetic particles after the active muon shield can be seen (Figure 21), without the additional particles created in the electromagnetic shield. The Figure 19 is a representation of all the particles going through the sensitive layers.

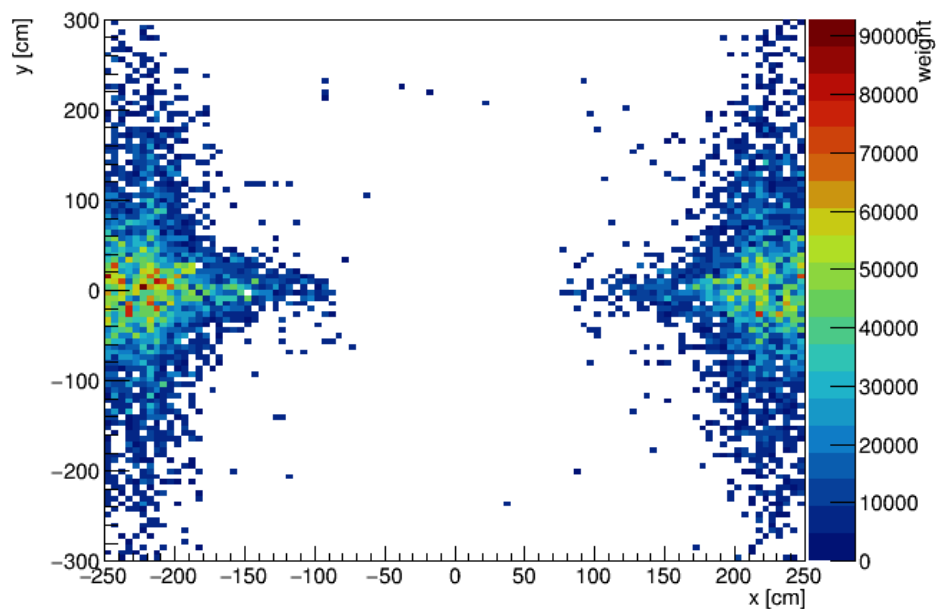


Figure 19: *Weighted number of particles crossing a box-shaped vacuum sensitive volume as a function of  $x$  and  $y$ . The events are weighted to one spill of  $4 \cdot 10^{13}$  POT.*

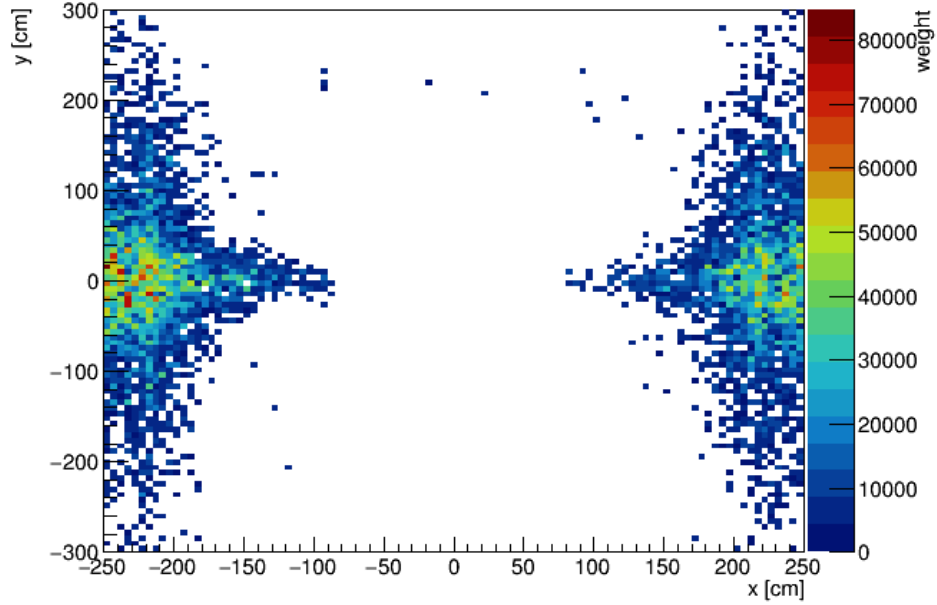


Figure 20: *Weighted number of muons crossing a box-shaped vacuum sensitive volume as a function of  $x$  and  $y$ . The events are weighted to one spill of  $4 \cdot 10^{13}$  POT.*

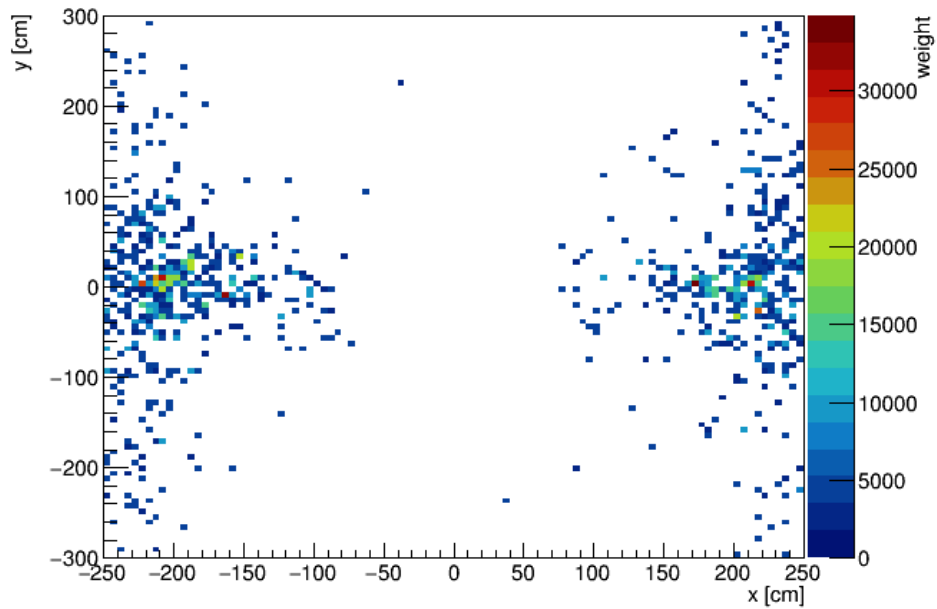


Figure 21: *Weighted number of electromagnetic particles crossing a box-shaped vacuum sensitive volume as a function of  $x$  and  $y$ . The events are weighted to one spill of  $4 \cdot 10^{13}$  POT.*

## B Code used

The code below describes how the lead boxes and trapezoids were defined to form the hour-glass shape. First the plate is defined and translated to its position. Then the trapezoid is defined and the matrix of translation and rotation is applied to it. The same process is then applied for the lower box and trapezoid.

```
TGeoVolume *plateup = gGeoManager->MakeBox("EmShieldbox", Lead, //
      fxSize1/2., (fySize1-ftrapregion1)/4., fzSize1/2.);
plateup->SetLineColor(kYellow);
AddSensitiveVolume(plateup);
fDetector->AddNode(plateup, 1, new TGeoTranslation( 0., //
      (fySize1+ftrapregion1)/4., fzPos1 )); //upper box
fDetector->AddNode(plateup, 1, new TGeoTranslation( 0., //
      (fySize1+ftrapregion1)/(-4.), fzPos1 )); //lower box
//set the matrix of rotation and translation for the upper trapezoid
TGeoRotation rotup;
TGeoTranslation transup;
rotup.RotateX(-90);
transup.SetTranslation( 0., ftrapregion1/4., fzPos1 );
TGeoCombiTrans combup(transup, rotup);
TGeoHMatrix *hmatup= new TGeoHMatrix(combup);

TGeoVolume *trapup = gGeoManager->MakeTrd2("EmShieldtrapup", Lead, //
      fXtrap1/2., fxSize1/2., fzSize1/2., fzSize1/2., ftrapregion1/4.);
trapup->SetLineColor(kYellow);
AddSensitiveVolume(trapup);
fDetector->AddNode(trapup, 1, hmatup ); //upper trapezoid
```

The code portion below presents how the layered design of Section 5 was defined. The hourglass shape is used and placed repeatedly with 1 mm of space between each layer. The sensitive vacuum layers will then be placed in between the lead plates.

```
Int_t NPlates=ftotallength/(fzSize1+0.1); //+ 0.1cm for the active layers
for(Int_t n=0; n<NPlates+1; n++)
{
  layered->AddNode(hourglass, n, new TGeoTranslation(0,0, //
      -ftotallength/2. +0.05 + (2*n+1)*(0.05 +fzSize1/2.)));
}
```

The different arguments to pass in the *geometry.config* file to generate the electromagnetic shield are presented below.

The parameters `emtrapheight` and `emtrapwidth` are used to set the trapezoids height and the width of the central region. `emrectheight` and `emwidth` are used to set the height

of the rectangular parts and `emthick` to set the thickness of the shield. The `zPos1` term positions the shield downstream of the active muon shield and upstream of the neutrino detector (at -34.89 m during the study).

```
c.EmShield = AttrDict(z=0*u.m)
c.EmShield.trapreg=emtrapheight*u.cm
c.EmShield.xSize1=emwidth*u.cm
c.EmShield.ySize1=2*emrectheight*u.cm+emtrapheight*u.cm
c.EmShield.zSize1=emthick*u.mm
c.EmShield.zPos1=0.5*(c.EmuMagnet.zC-c.EmuMagnet.Z/2.#
                    -c.decayVolume.length/2.-c.muShield.LE)
c.EmShield.xtrap1=emtrapwidth*u.cm
```

The two files below were used for HTCondor. The first one is a bash file used to simulate `NTOTAL` events with the `MuonBack` generator from the `MUONS` input file, separated in `NJOBS` jobs of `N` events. The thickness `Z` of the electromagnetic shield is passed from the `SUB` file.

In the file `run_simScript.py`, commands like `--EmShieldThickness` were added to easily pass the different parameters needed for the electromagnetic shield.

Once the simulation is over, the output files are transferred to an eos repository.

In the `SUB` file, the different parameters needed for the simulation are passed. The parameters needed to generate the geometry of the electromagnetic shield can be passed from a text file, which will be useful for the grid search optimisation of the shield.

```
#!/bin/bash
source /afs/cern.ch/user/a/algrandc/FairShipRun/config.sh
set -ux
echo "Starting script."
Z=$1
ProcId=$2
MUONS=/eos/experiment/ship/data/Mbias/#
pythia8_Geant4-withCharm_onlyMuons_4magTarget.root

NTOTAL=1000000
NJOBS=10
LSB_JOBINDEX=$((ProcId+1))
N=$((NTOTAL/NJOBS + (LSB_JOBINDEX == NJOBS ? NTOTAL % NJOBS : 0)))
FIRST=$(( (NTOTAL/NJOBS) * (LSB_JOBINDEX-1) ))
python2 "$FAIRSHIPRUN"/macro/run_simScript.py --MuonBack -f $MUONS #
--nEvents $N --EmShieldThickness $Z --firstEvent $FIRST --sameSeed 1 #
--seed 1

xrdcp ship.conical.MuonBack-TGeant4.root root://eospublic.cern.ch/#
eos/experiment/ship/user/algrandc/fiducial/noshield_emu/sim/ #
```

```
ship.conical.MuonBack-TGeant4-"$Z"_"$ProcId".root
if [ "$LSB_JOBINDEX" -eq 1 ]; then
    xrdcp geofile_full.conical.MuonBack-TGeant4.root root:// #
    eospublic.cern.ch//eos/experiment/ship/user/algrandc/ #
    fiducial/noshield_emu/geo/ #
    geofile_full.conical.MuonBack-TGeant4-"$Z".root
fi
```

```
executable = sim.sh
Arguments=$(Z) $(ProcId)
output = logs/sim.$(ProcId).out
error = logs/sim.$(ProcId).err
log = logs/sim.$(ProcId).log
requirements = (CERNEnvironment != "qa")
transfer_output_files = ""
+JobFlavour = "tomorrow"
request_memory= 2500KB
request_disk=60000KB
queue Z from file.txt
```